**Supporting information**

# A Portable Salivary 17β-Estradiol Sensor with Label-free Organic Field-effect Transistor

*Ziling Jiang, Guo Liu, Boya Zhang, Lianrui Cheng, Lianhong Shan, Enyu Zhang, Siyu Di, Chenyang Li, Dekai Ye, Fengjiao Zhang*

## 1. Experiment Details

### 1.1 Materials

PDPP2T-TT-OD was purchased from Sigma-Aldrich and stored at glove box before use. The DNA aptamer was designed and purchased from Sangon Biotech. The DNA sequence is HS-5'AAGGGATGCCGTTTGGGCCCAAGTTCGGCATAGTG-3' which was stored at −20 °C before use. Phosphate buffer saline (PBS) solution was prepared by mixing $Na_2HPO_4$ 2.2 g, $NaH_2PO_4$ 0.2 g, NaCl 8.5 g and 1000 mL $H_2O$ to get the 0.01 M PBS with pH= 7.4. The artificial saliva was purchased from sigma-Aldrich.

### 1.2 Fabrication of OFET biosensors.

OFET devices were fabricated on highly doped (*n*++) silicon wafer with a 300-nm $SiO_2$ oxide layer. The substrate was transferred into a glovebox after oxygen plasma treatment (80 W, 6 min) and immersed in a mixture of octadecyltrichlorosilane (50 μL, Sigma) and trichloroethylene (50 mL, Sigma-Aldrich) to achieve a self-assembled monolayer on the $SiO_2$. Cr/Au (5/25 nm) source-drain electrodes were thermally evaporated as the patterned source and drain electrodes, with a channel length and width of 100 μm and 6100 μm, respectively. In order to enhance the solution operation stability of OFET sensor, the source and drain electrodes were modified by being exposed to perfluorohexylethanethiol (10 mM in ethanol), via Au-S self-assembling bonding for 1 h. After washing with ethanol twice, the PDPP2T-TT-OD film was deposited from chloroform solution (5 mg/mL) at 5000 r.p.m. for 60 s following an on-the-fly-dispensing spin coating method.[1] Subsequently, the samples were annealed for 30 min on a hotplate at 160 °C. The thickness of OSC film was 12.3±0.85 nm.

### 1.3 Immobilization of DNA aptamer for biosensors

To construct an aptamer-based OFET biosensor, the thiol-DNA aptamer molecules were immobilized on PDPP2T-TT-OD film, mediated by the gold nanoparticle pre-deposited on the OSC layer. The detailed procedure is as follows: At first, gold nanoparticles with a thickness of 1.5 nm were deposited on the surface of semiconductor films by vacuum thermal deposition process. DNA aptamer was dissolved by Milli Q water (with pH of 7) at a concentration of 10 μM, followed by

being heated up to 95 °C for 5 min and then cooled at 4 °C for 30 min. Finally, the OFET device (with a size of 1 $cm^2$) was exposed to 50 μL DNA aptamer solution for 1 h. The reaction was carried out at room temperature.

### 1.4 Characterization of the electrical performance

All measurements were performed under ambient conditions at room temperature. The source-drain voltage ($V_{DS}$) and gate voltage ($V_{GS}$) were applied to the electrodes while measuring the source-drain current ($I_{DS}$) with Keithley SCS 4200. For electrical testing in aqueous environments, a polydimethylsiloxane (PDMS) well was placed on top of the channels and filled with 20 μL of PBS solution. The transfer curve of the OFET was obtained by measuring $I_{DS}$ versus $V_{GS}$ ranging from 10 to −30 V with a step of 0.5 V, under a $V_{DS}$ of −1 V. The output curve of the OFET was obtained by measuring $I_{DS}$ versus $V_{DS}$ ranging 0 to −2 V with 0.02 V steps, and applied the $V_{GS}$ from 0 to −30 V with 5 V steps.

For the real-time sensing measurements, the $I_{DS}$ was continuously monitored under a fixed operation voltage. To trigger the sensing response, 2 μL of target 17-β estradiol solution was added into the PDMS cell. For calibration, a series of target solutions with varying concentration were prepared, and the corresponding device responses were recorded sequentially from the most diluted to the most concentrated sample. It should be note that, a new device is used for each detection measurement. The normalized response $\Delta I/I_0$ of the sensor was calculated according to $(I_t\text{-}I_0)/I_0$, where $I_t$ and $I_0$ represent the real-time current and the baseline current, respectively.

According to the guidelines of the International Union of Pure and Applied Chemistry, the limit of detection (LOD) was calculated following the equation:

$$\mathrm{LOD}=\frac{\left(\frac{\Delta I}{I_0}\pm 3\delta\right)-a}{b}$$

where $\frac{\Delta I}{I_0}$ represents the average response of the blank sample, δ is the relative standard

deviation. The $\left(\frac{\Delta I}{I_0} \pm 3\delta\right)$ was obtained from the relative current variation in the negative control sensors. In the expression, *a* and *b* are the intercept and slope of the calibration curve, respectively.

### 1.5 Surface characterization

The topographic morphology of semiconductor film under various treatments was analyzed using an atomic force microscope (AFM, Bruker Dimension Icon) operating in tapping mode in air. Moreover, the surface potentials of the corresponding films were investigated by Kelvin probe force microscopy (KPFM) with an SCM-PIT-V2 tip 100 nm away from the film surface in the air. UPS and XPS measurements were performed with a Kratos ULTRA AXIS DLD photoelectron spectroscopy system under an ultrahigh vacuum of $3\times10^{-9}$ Torr, for surface potential and elements analysis, respectively. The excitation is generated with He-discharge lamp (21.22 eV) for UPS and monochromatic Al Kα X-ray (1486.6 eV) excitation sources for XPS analysis, respectively. A bias voltage of –9 V was applied to the sample to obtain the cutoff (SECO) region of secondary electrons. The Fermi edge was calibrated from the UPS spectrum of the $Ar^+$-sputtered clean Au substrate and was referred to as the zero-binding energy to normalize the UPS and XPS spectra.

## 2. Supplementary Figures and Tables

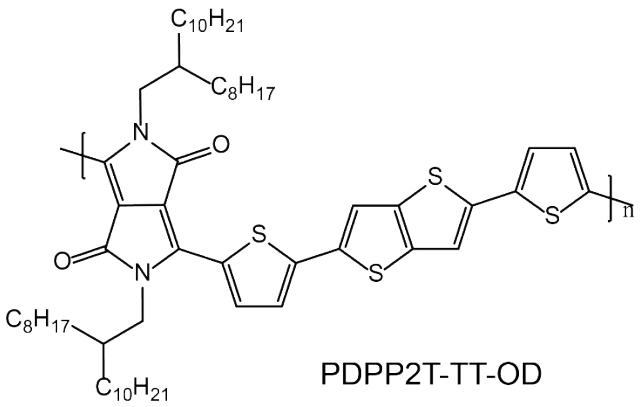


Figure S1. The molecular structure of PDPP2T-TT-OD.

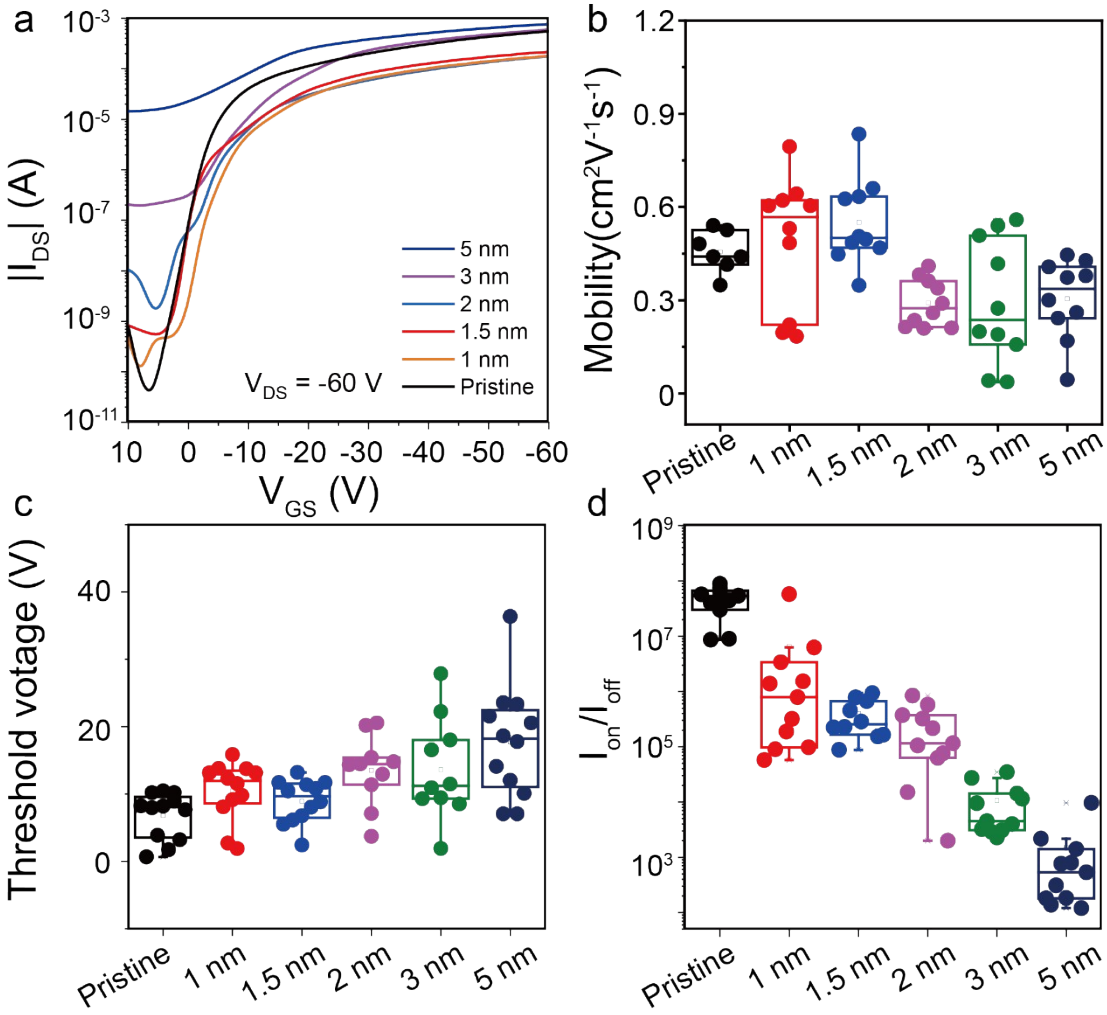


Figure S2. (a) transfer curves of pristine PDPP2T-TT-OD and w/ 1nm, 1.5 nm, 2 nm, 3 nm, 5 nm Au nanoparticles on the film. (b), (c), and (d). The calculated mobility, threshold voltage and current ration of pristine PDPP2T-TT-OD and w/ 1nm, 1.5 nm, 2 nm, 3 nm, 5 nm Au nanoparticles on the film.

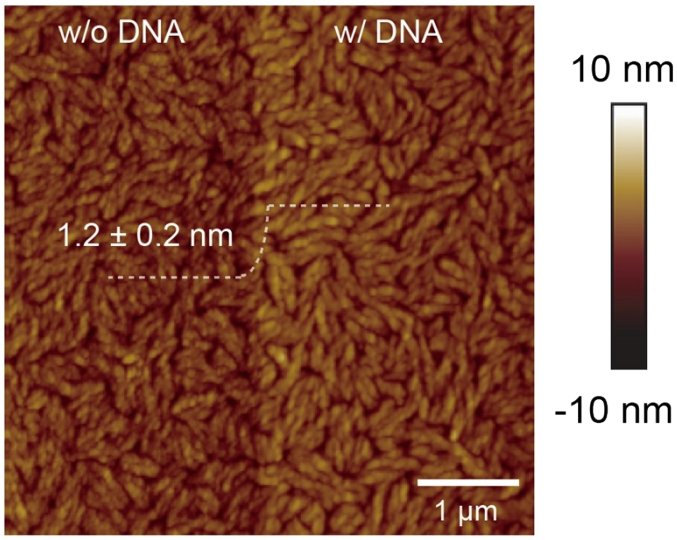


Figure S3. Morphology of surface characterization. AFM image of PDPP2T-TT-OD/Au film w/o and w/ DNA aptamer immobilization. After immobilized DNA aptamer, the thickness increased 1.2 ± 0.2 nm.

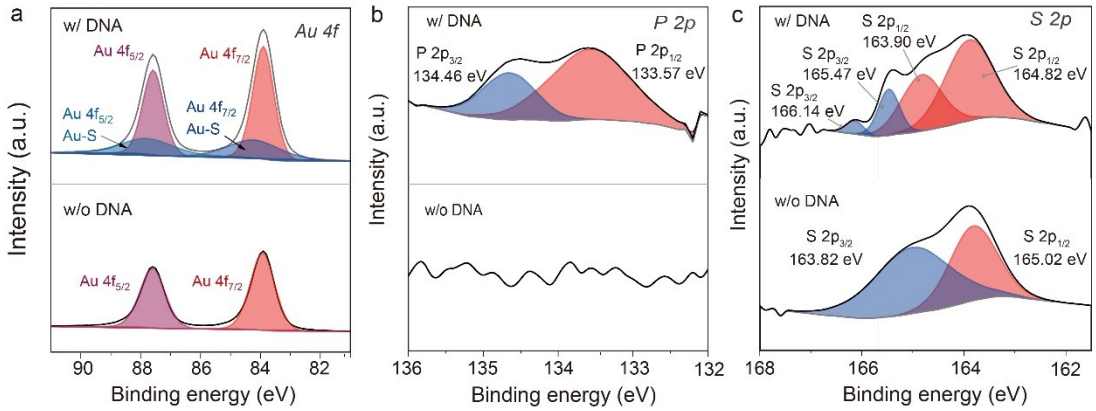


Figure S4. XPS characterization. High-resolution (a) Au *4f*, (b) P *2p* and (c) S *2p* XPS spectra of pristine DPP-TT-OD/Au film and DPP-TT-OD/Au film with DNA modification.

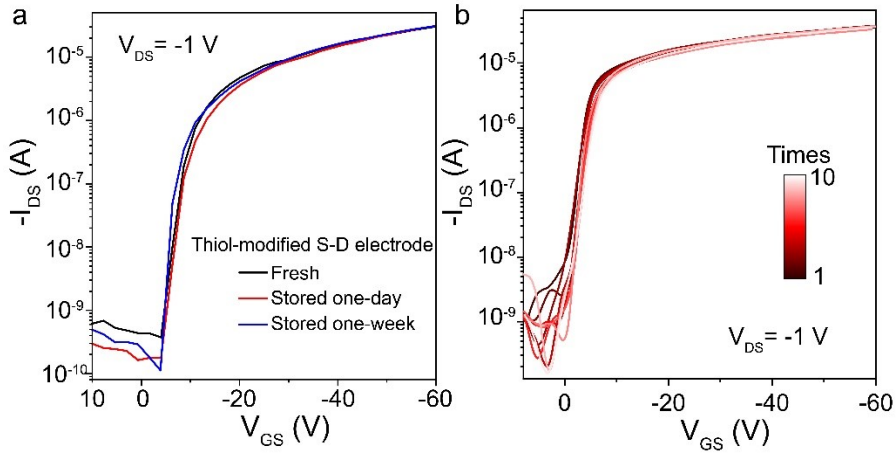


Figure S5. (a) Transfer characterization of PDPP2T-TT-OD based OFET fabricated using source and drain electrodes immediately after PFHET modification, as well as electrodes stored for one day and one week after modification. (a) Repeated transfer characterization of PDPP2T-TT-OD based OFET.

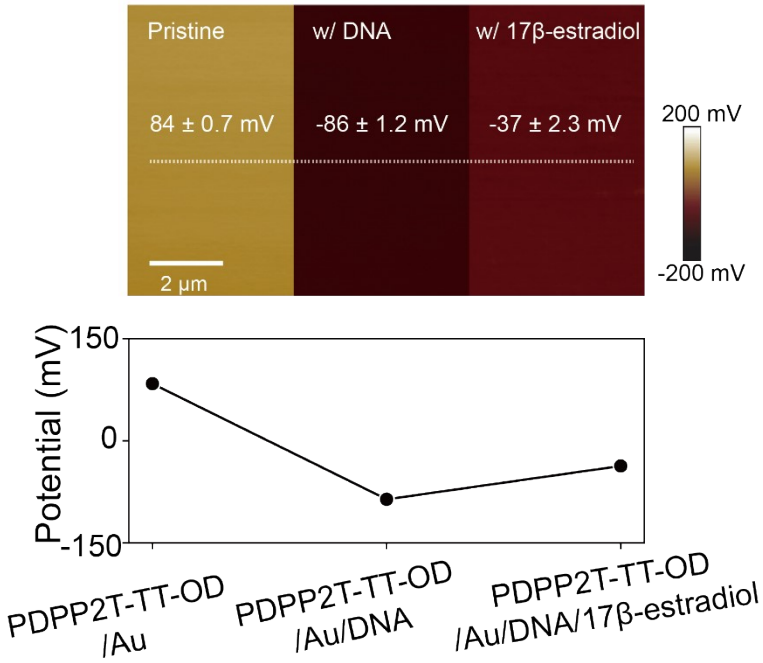


Figure S6. KPFM characterization. Surface potential change of PDPPTT-2T-OD/Au film, w/ DNA aptamer functionalization and interaction with 17β-estradiol.

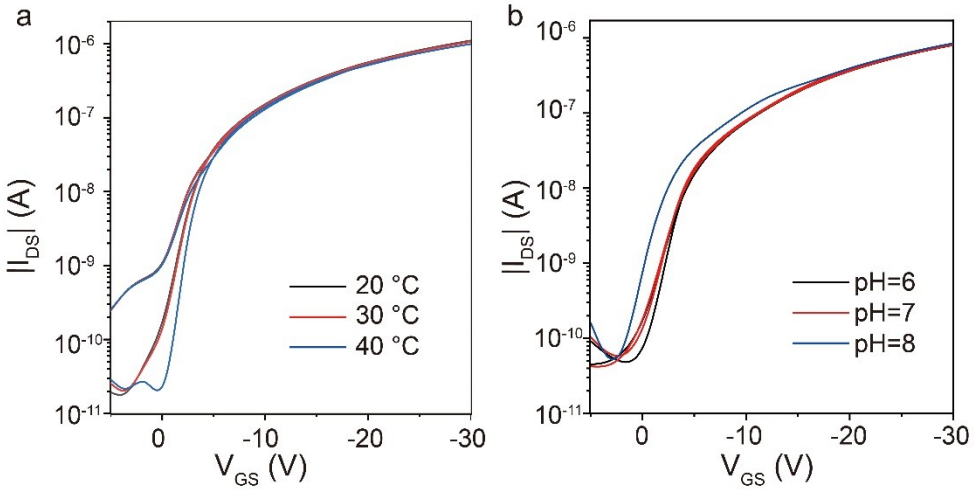


Figure S7. The transfer curves characterization of DNA aptamer functionalized OFET biosensors with (a) different temperature and (b) different pH value. The $V_{DS}$ was set as –1 V.

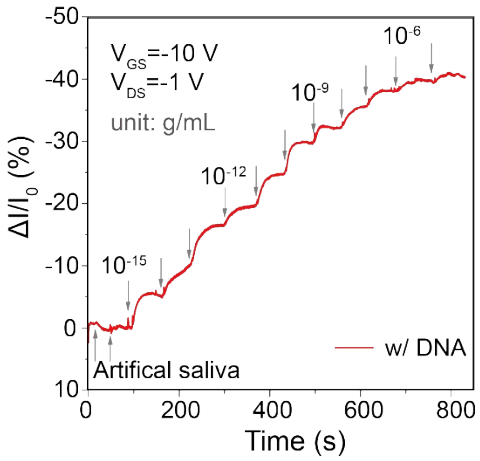


Figure S8. Real-time current response of the DNA-aptamer functionalized OFET to 17β-estradiol in saliva.

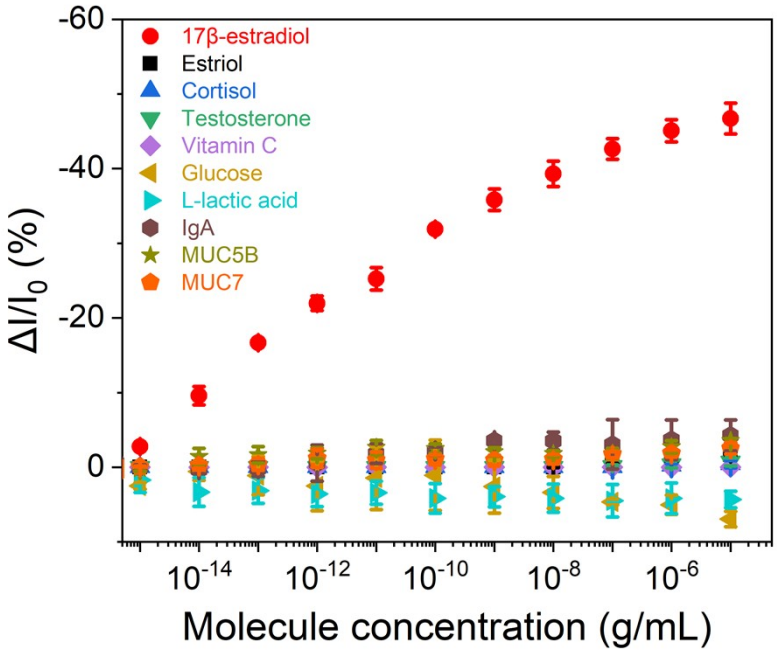


Figure S9. The current response of DNA aptamer functionalized OFET to different biomolecules in saliva. A series of interferents present in real saliva, including representative steroids (estriol, cortisol, and testosterone), proteins (IgA, MUC5B, and MUC7), and metabolic components (glucose and L-lactic acid), were tested using the DNA-aptamer-based OFET to evaluate its response to these species.

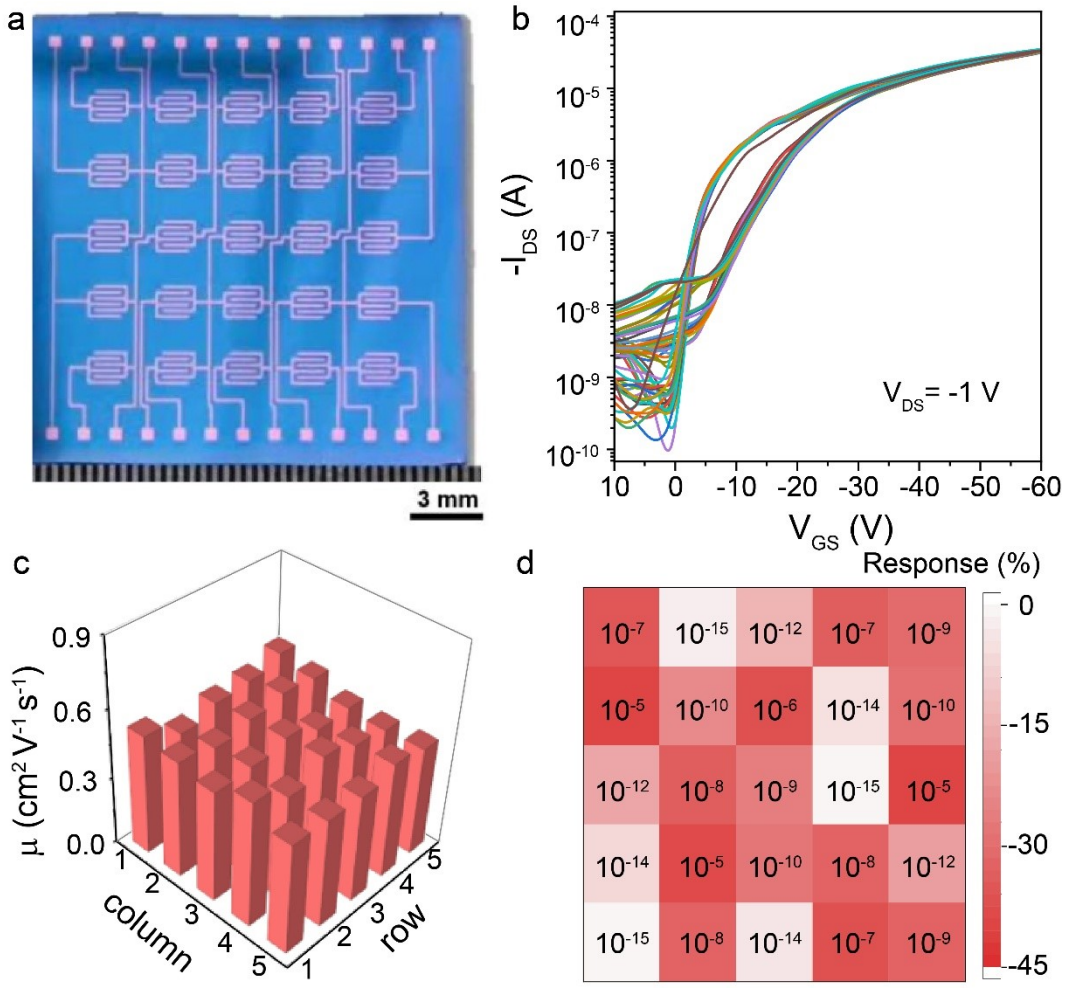


Figure S10. (a) Photograph of an OFET based sensor array consisting of 5×5 devices fabricated on Si/$SiO_2$ substrate. (b-c) Transfer curves (b) and extracted mobilities (c) of the 25 OFET devices within one array. (d) Signal responses of the OFET sensor array to 17β-estradiol. All devices were fabricated with thiol-modified source-drain electrodes, and DNA-aptamer functionalized channel.

Table S1. A comparison of reported biosensors for OFET device

| No. | Recognition element | Transducing method | Limit of detection | Response time | Linear range | Sample | reference |
|---|---|---|---|---|---|---|---|
| 1 | Antibody | Electrochemical | 6 pg/mL | 30 min | 6-1200 pg/mL | Blood serum | 2 |
| 2 | | Fluorescence immune assay | $6.37\times10^{-6}$ ng/mL | 180 min | $1\times10^{-5}$-1 ng/mL | Human urine | 3 |
| 3 | | Optical (SPR) | 3 pg/mL | 180 min | 3-$10^5$ pg/mL | Tap water | 4 |
| 4 | | Electrochemical | 0.84 pg/mL | 55 min | 0.84-$1.36\times10^4$ pg/mL | Bovine serum | 5 |
| 5 | | SERS | 0.0136 pg/mL | 25 min | 0.0272 pg/mL-2.72 ng/mL | Environmental water | 6 |
| 6 | MIPs | HPLC | 1.26 ng/mL | 360 min | 1.26-3.22 ng/mL | Human urine | 7 |
| 7 | | Electrochemical | $1.86\times10^2$ ng/mL | 0.6 min | $0.272\times10^2$-$2.18\times10^2$ ng/mL | Water | 8 |
| 8 | | Optical (SPR) | $0.68\times10^{-4}$ ng/mL | 10 min | $0.68\times10^{-4}$-0.68 ng/mL | Water | 9 |
| 9 | | HPLC | 4.81 mg/L | 720 min | 4.81-16.03 mg/L | Goat milk | 10 |
| 10 | Estrogen receptor | - | $0.272\times10^{-4}$ ng/mL | 90 min | $0.272\times10^{-4}$-0.272 ng/mL | Buffer | 11 |

| | | | | | | | |
|---|---|---|---|---|---|---|---|
| 11 | Aptamer | Optical | 0.6 ng/mL (2.1 nM) | 4 min | 5 nM—75 nM | Environmental water | [12] |
| 12 | | Electrochemical | 0.217 ng/mL | 40 min | $0.272\times10^{-3}$-0.16 ng/mL | Environmental water | [13] |
| 13 | | SERS | $0.75\times10^{-6}$ ng/mL | 30 min | $0.272\times10^{-4}$-0.272 ng/mL | Aquatic water | [14] |
| 14 | | Optical (SPR) | 25 pg/mL | 8 min | - | Aqueous media | [15] |
| 15 | | FRET | 0.1 ng/mL | 120 min | 0.1 ng/mL-10 mg/mL | Environmental water | [16] |
| 16 | | OFET | 0.27 fg/mL | 0.4 min | 0.1 fg/mL-10 μg/mL | Saliva | **This work** |

## References


1 F. J. Zhang, C. A. Di, N. Berdunov, Y. B. Hu, X. K. Gao, Q. Meng, H. Sirringhaus and D. B. Zhu, Ultrathin Film Organic Transistors: Precise Control of Semiconductor Thickness via Spin-Coating, *Adv. Mater.* 2013, **25**, 1401-1407.

2 X. Liu and D. Wong, Picogram-detection of estradiol at an electrochemical immunosensor with a gold nanoparticle|Protein G-(LC-SPDP)-scaffold, *Talanta* 2009, **77**, 1437-1443.

3 L. Du, W. Ji, Y. Zhang, C. Zhang, G. Liu and S. Wang, An ultrasensitive detection of 17β-estradiol using a gold nanoparticle-based fluorescence immunoassay, *The Analyst* 2015, **140**, 2001-2007.

4 A. Minopoli, N. Sakač, B. Lenyk, R. Campanile, D. Mayer, A. Offenhäusser, R. Velotta and B. Della Ventura, LSPR-based colorimetric immunosensor for rapid and sensitive 17β-estradiol detection in tap water, *Sens. Actuator B Chem.* 2020, **308**.

5 M. J. Monerris, F. J. Arévalo, H. Fernández, M. A. Zon and P. G. Molina, Development of a very sensitive electrochemical immunosensor for the determination of 17β-estradiol in bovine serum samples, *Sens. Actuator B Chem.* 2015, **208**, 525-531.

6 S. Liu, R. Cheng, Y. Chen, H. Shi and G. Zhao, A simple one-step pretreatment, highly sensitive and selective sensing of 17β-estradiol in environmental water samples using surface-enhanced Raman spectroscopy, *Sens. Actuator B Chem.* 2018, **254**, 1157-1164.

7 R. Gadzała-Kopciuch, J. Ričanyová and B. Buszewski, Isolation and detection of steroids from human urine by molecularly imprinted solid-phase extraction and liquid chromatography, *J. Chromatogr. B* 2009, **877**, 1177-1184.

8 S. Des Azevedo, D. Lakshmi, I. Chianella, M. J. Whitcombe, K. Karim, P. K. Ivanova-Mitseva, S. Subrahmanyam and S. A. Piletsky, Molecularly Imprinted Polymer-Hybrid Electrochemical Sensor for the Detection of β-Estradiol, *Ind. Eng. Chem. Res.* 2013, **52**, 13917-13923.

9 Y. Tan and T. Wei, Detection of 17β-estradiol in water samples by a novel double-

layer molecularly imprinted film-based biosensor, *Talanta* 2015, **141**, 279-287.

10 H. Xiong, X. Wu, W. Lu, J. Fu, H. Peng, J. Li, X. Wang, H. Xiong and L. Chen, Switchable zipper-like thermoresponsive molecularly imprinted polymers for selective recognition and extraction of estradiol, *Talanta* 2018, **176**, 187-194.

11 B. K. Kim, J. Li, J.-E. Im, K.-S. Ahn, T. S. Park, S. I. Cho, Y.-R. Kim and W.-Y. Lee, Impedometric estrogen biosensor based on estrogen receptor alpha-immobilized gold electrode, *J. Electroanal. Chem.* 2012, **671**, 106-111.

12 N. Yildirim, F. Long, C. Gao, M. He, H.-C. Shi and A. Z. Gu, Aptamer-Based Optical Biosensor For Rapid and Sensitive Detection of 17β-Estradiol In Water Samples, *Environ. Sci. Technol.* 2012, **46**, 3288-3294.

13 L. Fan, G. Zhao, H. Shi and M. Liu, A simple and label-free aptasensor based on nickel hexacyanoferrate nanoparticles as signal probe for highly sensitive detection of 17β-estradiol, *Biosens. Bioelectron.* 2015, **68**, 303-309.

14 H. Pu, X. Xie, D.-W. Sun, Q. Wei and Y. Jiang, Double strand DNA functionalized Au@Ag Nps for ultrasensitive detection of 17β-estradiol using surface-enhanced raman spectroscopy, *Talanta* 2019, **195**, 419-425.

15 J. S. Mitchell, Y. Wu, C. J. Cook and L. Main, Estrogen conjugation and antibody binding interactions in surface plasmon resonance biosensing, *Steroids* 2006, **71**, 618-631.

16 G. Zhang, T. Li, J. Zhang and A. Chen, A simple FRET-based turn-on fluorescent aptasensor for 17β-estradiol determination in environmental water, urine and milk samples, *Sens. Actuator B Chem.* 2018, **273**, 1648-1653.